ELSEVIER

Journal of Alloys and Compounds 293–295 (1999) 417–420

Journal of ALLOYS AND COMPOUNDS

Hydrogen absorption and desorption properties of Hf-based intermetallic compounds

D. Mukai[a], H. Miyata[b], K. Aoki[b,]*

[a]Graduate School, Kitami Institute of Technology, present address, Mitsui Mining & Smelting Co., Ltd., Takehara, Hiroshima 725-0025, Japan
[b]Kitami Institute of Technology, 165 Koencho, Kitami, Hokkaido 090-8507, Japan

Abstract

Hydrogen absorption and desorption properties of Hf-based intermetallic compounds were studied by high pressure differential scanning calorimetry (DSC) in an H_2 atmosphere and the Sieverts method. Structural changes were examined by powder X-ray diffractometry (XRD). The PCT curves of HfNi and HfCo showed the pressure plateau due to the formation of $HfNiH_3$ and $HfCoH_3$ with the CrB(B_f) type hydride, respectively. Hydrogen was absorbed forming a solid solution in Hf_2Fe, Hf_2Co, Hf_2Ni, Hf_2Cu, Hf_2Pd, HfPd, HfV_2, $HfCr_2$, $HfMn_2$ and $HfMo_2$. On the other hand, no hydrogen absorption was detected in $HfFe_2$, $HfCo_2$ and $HfPd_2$.

Keywords: Hf based intermetallics; Hydrogen absorption; PCT curves

1. Introduction

As is commonly known, hydrogen absorption alloys are mainly intermetallic compounds consisting of hydride forming metals such as 2A, 3A or 4A group elements and hydride non-forming metals such as 7A or 8A group elements and having specific crystal structure such as $CaCu_5$, $MgZn_2$ and so on. So far, hydrogen absorption and desorption properties of intermetallic compounds containing Mg (2A), rare earth metals (3A) and Ti, Zr (4A metals) have been extensively investigated. RNi_5 alloys have received practical application as a negative electrode in MH battery. Many methods have been proposed to develop new and high performance hydrogen absorption alloys. We consider that a guide principle to design new hydrogen absorption alloys may be derived by comparing hydrogen absorption properties among same group alloys. We paid attention to intermetallic compounds containing 4A elements. In the present work, the hydrogen absorption and desorption properties of Hf-based intermetallics are investigated in order to compare them with those of Ti and Zr based intermetallics.

2. Experimental

Hf_2M, HfM and HfM_2 (M=V, Cr, Mn, Fe, Co, Ni, Cu, Mo and Pd) compounds were prepared by arc melting in an argon atmosphere. These compounds were homogenized at 1273 K for 253 ks in vacuum and pulverized into 50 mesh under powder. Powder samples were thermally analyzed using a differential scanning calorimeter (DSC) at a heating rate of 30 K/min in an H_2 (7 N) atmosphere. They were also reacted with 5 MPa H_2 (7N) isothermally for 43 ks between 298 and 573 K. Crystal structures of the powder samples before and after hydrogenation were identified with the powder X-ray diffractometer (XRD) using the Cu Kα radiation. Pressure–composition–temperature (PCT) relationships were measured by the Sieverts method. The morphology of the samples before and after 100 hydrogen absorption–desorption cycles was observed by scanning electron microscopy (SEM).

3. Results and discussion

Table 1 shows the intermetallic compounds obtained in the Hf–M systems and their crystal structures. 15 intermetallic compounds are formed in 27 Hf–M compositions, and the other 12 samples form the solid solution alloy. The low temperature phases, i.e. $HfMn_2$ (C14), $HfFe_2$ (C36) and $HfMo_2$ (C15) are formed among the Laves phases in

---

*Corresponding author.

0925-8388/99/$ – see front matter
PII: S0925-8388(99)00456-9

Table 1
The intermetallic compounds obtained in the Hf–M systems and their crystal structures

Elements (M)	Hf_2M	HfM	HfM_2
V	–	–	HfV_2 (C15)
Cr	–	–	$HfCr_2$ (C14)
Mn	–	–	$HfMn_2$ (C14)
Fe	Hf_2Fe (Ti_2Ni type)	–	$HfFe_2$ (C36)
Co	Hf_2Co (Ti_2Ni type)	HfCo(B2)	$HfCo_2$ (C15)
Ni	Hf_2Ni (C16)	HfNi(B_f)	–
Cu	Hf_2Cu($C11_b$)	–	–
Mo	–	–	$HfMo_2$ (C15)
Pd	Hf_2Pd ($C11_b$)	HfPd (?)	$HfPd_2$ ($C11_b$)

the present experimental conditions. The crystal structure of Hf_2Co is not $E9_3$, but is identified with the Ti_2Ni type one [1]. The crystal structures of the other compounds are in good agreement with the phase diagrams [1]. By comparing the phase diagrams of Ti, Zr and Hf based alloys, it is found that A_2 (=Ti, Zr and Hf) Cu, A_2Pd, ACo, AMn_2, ACo_2 and APd_2 form compounds having the same crystal structures. Both ZrNi and HfNi, both ZrV_2 and HfV_2 take the same crystal structures, respectively. However, the other compounds take different crystal structures.

The powder samples were thermally analyzed using DSC in an H_2 atmosphere in order to grasp the outline of hydrogen absorption and desorption properties of all compounds. As an example, Fig. 1 shows DSC curves of HfNi heated in 0.2–5.0 MPa H_2. The DSC curves show a sharp exothermic peak resulting from hydrogen absorption during cooling. They show a sharp endothermic peak resulting from hydrogen desorption during heating. Since the sharp exothermic and endothermic peak correspond to the formation and decomposition of hydride respectively, the PCT curve of HfNi is expected to exhibit a pressure plateau.

Fig. 2 shows the PCT curves of HfNi. The pressure plateau is clearly observed at about 0.15 MPa (absorption) and about 0.07 MPa (desorption) at 423 K. The plateau pressure increases as the temperature goes up, and the plateau disappears above 573 K.

Fig. 3 shows X-ray diffraction (XRD) patterns of HfNi hydrogenated isothermally for 43 ks between 298 and 573 K. The XRD patterns of the original and hydrogenated samples are indexed on the basis of HfNi and $HfNiH_3$ with the CrB (B_f) type structure in good agreement with the previous report [2]. Therefore, the pressure plateau (Fig. 2) is concluded to result from the formation of $HfNiH_3$. The DSC curves of HfCo also show the sharp endothermic and exothermic peaks, but those of Hf_2Fe, Hf_2Co, Hf_2Ni, Hf_2Cu, Hf_2Pd, HfPd, HfV_2, $HfCr_2$, $HfMn_2$ and $HfMo_2$ show the broad exothermic and endothermic peaks. Therefore, it is expected that the PCT curves of HfCo show the pressure plateau, but the others do not. Practically, the PCT curves of HfCo show the pressure plateau below 573 K. The XRD patterns of the original and hydrogenated HfCo are indexed on the basis of HfCo with the B2 structure and $HfCoH_3$ with the Cr (B_f) structure [1], respectively, which

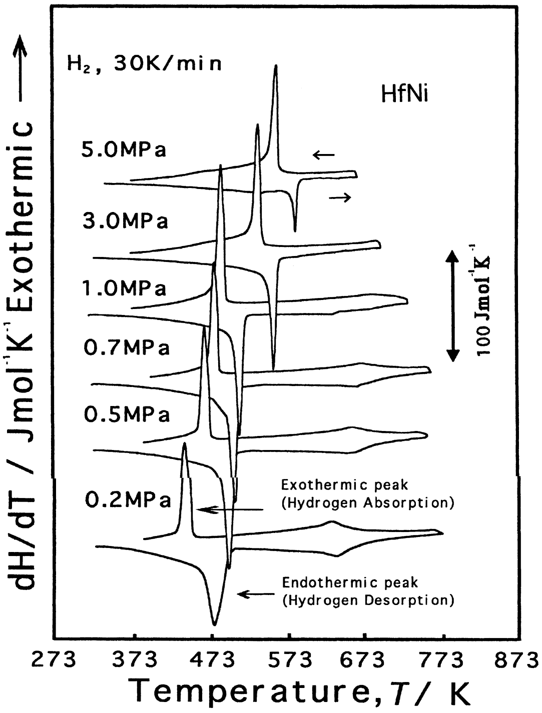

Fig. 1. DSC curves of HfNi heated in 0.2–5.0 MPa H_2.

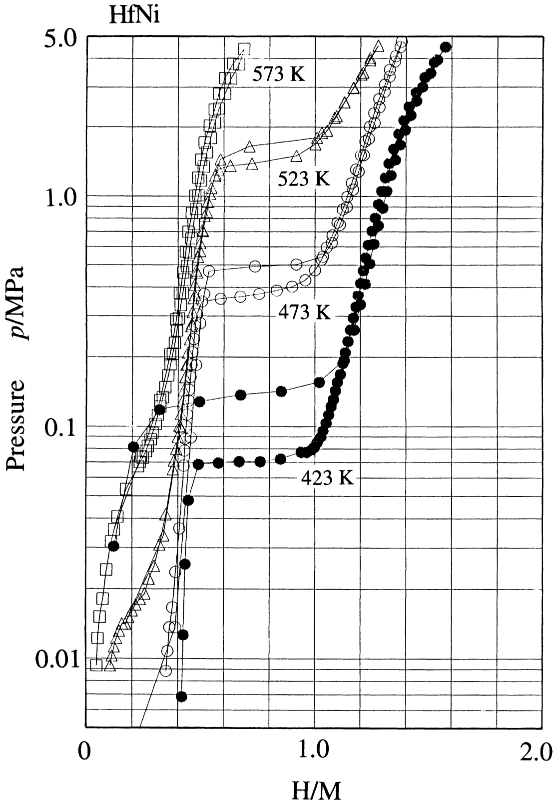

Fig. 2. The PCT curves of hydrogen absorption and desorption for HfNi.

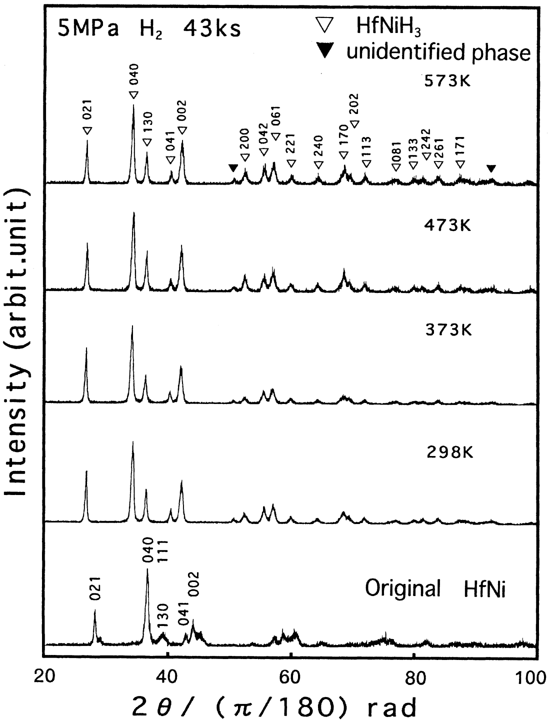

Fig. 3. XRD patterns of HfNi hydrogenated between 293 K and 573 K for 43 ks.

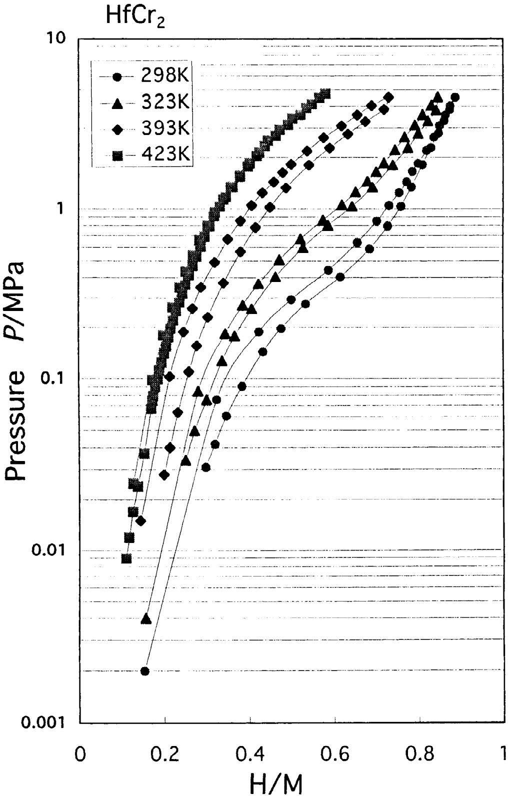

Fig. 4. The PCT curve for hydrogen absorption and desorption of $HfCr_2$.

indicates that the pressure plateau results from the formation of $HfCoH_3$.

The PCT curves of Hf_2Fe, Hf_2Co, Hf_2Ni, Hf_2Cu, Hf_2Pd, HfPd, HfV_2, $HfCr_2$, $HfMn_2$ and $HfMo_2$ do not show the pressure plateau. As an example, Fig. 4 shows the PCT curves of $HfCr_2$ (C14). These PCT curves do not show the pressure plateau and the hydrogen pressure increases with the increasing of the hydrogen content, which indicates the formation of a solid solution alloy.

Fig. 5 shows SEM of HfNi and $HfCr_2$ before and after 100 hydrogen absorption–desorption cycles. The size and morphology of $HfCr_2$ powder does not substantially change by hydrogenation, but the size of HfNi powder is reduced by 100 hydrogen absorption–desorption cycles. Therefore, it is concluded that the formation of metal hydride gives rise to the reduction of the powder size, while the formation of solid solution does not change the powder size.

Table 2 summarizes the crystal structures of Hf-based intermetallic compounds before and after hydrogenation, the maximum amount of absorbed hydrogen and the states of hydrogen absorption. This table indicates that the most amount of hydrogen, i.e. about 1.5(H/M) is absorbed in the HfM compounds (HfNi and HfCo) which form the metal hydride with the CrB (B_f) type structure. Intermediate amount of hydrogen, i.e. between 0.71 and 1.13(H/M) is absorbed forming the solid solution in the Hf_2M (Ti_2Ni type, M=Fe, Co, Ni) and HfM_2 (Laves type structure, M=V, Cr, Mn). On the contrary, a small amount of hydrogen, i.e. between 0.28 and 0.49(H/M) is absorbed in the Hf_2M ($C11_b$ type, M=Cu, Pd), HfPd and $HfMo_2$ (C15). No hydrogen absorption is observed in $HfFe_2$ (C36), $HfCo_2$ (C15) and $HfPd_2$ ($C11_b$). The present work indicates that the intermetallic compounds, which form metal hydride, absorb most hydrogen and are promising as hydrogen absorption alloys. Ti_2Ni type compounds and Laves compounds absorb much hydrogen. On the contrary, it is considered that $C11_b$ compounds are inappropriate for hydrogen absorption alloys.

4. Summary and conclusion

Hydrogen absorption properties of Hf_2M, HfM and HfM_2 (M=V, Cr, Mn, Fe, Co, Ni, Cu, Mo and Pd) compounds were studied by a high pressure differential scanning calorimeter (DSC) in a hydrogen atmosphere and the Sieverts method. Structural changes were studied by powder X-ray diffractometry (XRD). The metal hydride $HfNiH_3$ and $HfCoH_3$ with the B_f type structure are formed by hydrogenation HfNi and HfCo, respectively and the PCT curves of these compounds show the pressure plateau. The maximum hydrogen absorption capacity of HfCo and HfNi compound is 1.5(H/M) and 1.6 (H/M) respectively. Hydrogen is absorbed forming a solid solution alloy in Hf_2Fe (Ti_2Ni type), Hf_2Co (Ti_2Ni type), Hf_2Ni (C16),

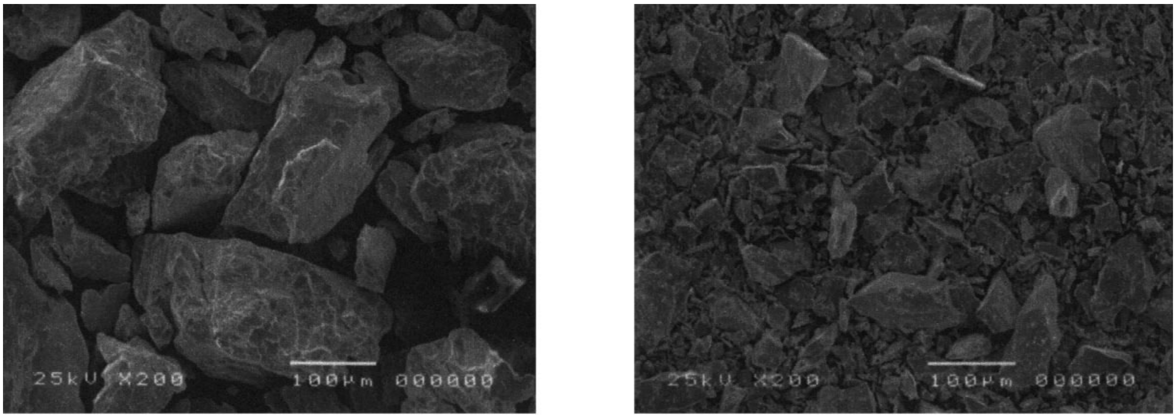

(a) NiHf before hydrogen absorption

(a) Cr_2Hf before hydrogen absorption

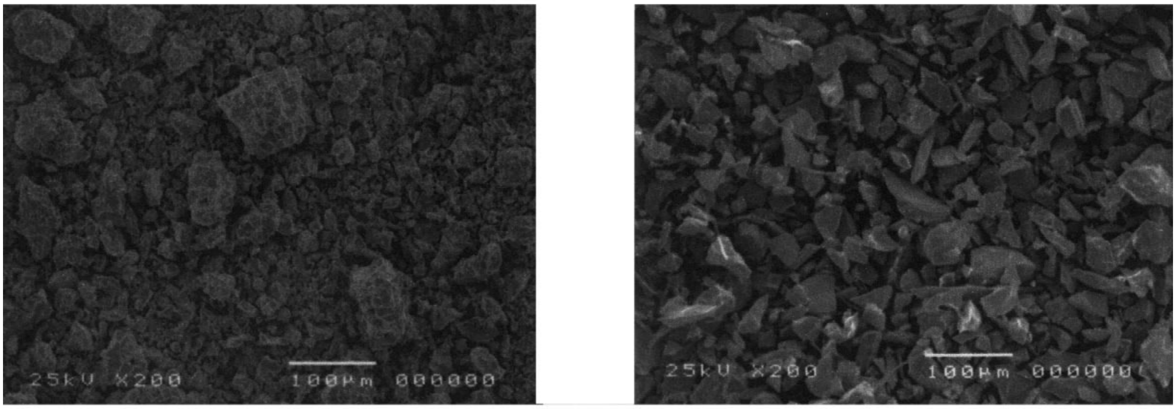

(b) NiHf after 100 cycles

(b) Cr_2Hf after 100 cycles

Fig. 5. Scanning electron micrographs (SEM) before and after 100 cycles hydrogen Absorption and desorption in HfNi and $HfCr_2$.

Hf_2Cu (C11_b), Hf_2Pd (C11_b), HfV_2 (C15), $HfCr_2$ (C14), $HfMn_2$ (C14), $HfMo_2$ (C15) and HfPd (unknown). On the contrary, no hydrogen absorption is detected in the $HfFe_2$ (C36), HfCo2 (C15) and $HfPd_2$ (C11_b) compounds.

Table 2
Hydrogen absorption properties of Hf-based intermetallic compounds

Alloys (original)	After H_2 absorption	Maximum H_2 (H/M)	States
Hf_2Fe (Ti_2Ni type)	Hf_2FeH_x (Ti_2Ni type)	1.13	S.S
Hf_2Co (Ti_2Ni type)	Hf_2CoH_x (Ti_2Ni type)	0.95	S.S
Hf_2Ni (Ti_2Ni type)	Hf_2NiH_x (Ti_2Ni type)	0.92	S.S
Hf_2Cu (C11_b)	Hf_2CuH_x (C11_b)	0.49	S.S
Hf_2Pd (C11_b)	Hf_2PdH_x (C11_b)	0.39	S.S
HfCo (B2)	$HfCoH_3$ (B_f)	1.53	M.H
HfNi (B_f)	$HfNiH_3$ (B_f)	1.58	M.H
HfPd (?)	$HfPdH_x$ (?)	0.35	S.S
HfV_2 (C15)	HfV_2H_x (C15)	0.81	S.S
$HfCr_2$ (C14)	$HfCr_2H_x$ (C14)	0.90	S.S
$HfMn_2$ (C14)	$HfMn_2H_x$ (C14)	0.71	S.S
$HfFe_2$ (C36)	–	–	–
$HfCo_2$ (C15)	–	–	–
$HfMo_2$ (C15)	$MfMo_2H_x$ (C15)	0.28	–
$HfPd_2$ (C11_b)	–	–	–

Acknowledgements

This work was supported in part by a Grant-in-aid for Scientific Research on Priority Areas A of 'New Protium Function' from the Ministry of Education, Science, Sports and Culture.

References

[1] T.B. Massalsky, Binary Alloy Phase Diagrams, ASM International, Material Park, OH, 1990.
[2] R.M. van Essen, K.H.J. Buschow, J. Less-Comm. Met. 64 (1979) 277.